PROTEINS: Structure, Function, and Genetics 17:1–10 (1993)

RESEARCH ARTICLES

Automated Docking in Crystallography: Analysis of the Substrates of Aconitase

David S. Goodsell,[1] Hans Lauble,[2] C. David Stout,[2] and Arthur J. Olson[2]
[1]*Molecular Biology Institute, University of California, Los Angeles, Los Angeles, California 90024; and*
[2]*Department of Molecular Biology, The Scripps Research Institute, La Jolla, California 92037*

ABSTRACT **Automated docking of substrates to proteins of known structure aids the process of crystallographic analysis in two ways. First, automated docking can be used to generate a small number of starting models for substrates using only protein coordinates from an early stage of refinement. Second, automated docking provides a method for exploring aspects of catalysis that are inaccessible to crystallography by postulating binding modes of catalytic intermediates. This paper describes the use of automated docking to explore the binding of substrates to aconitase. The technique starts with a substrate molecule in an arbitrary configuration and position and finds favorable docked configurations in a (static) protein active site based on a molecular mechanics type force field. Using protein coordinates from an early stage of refinement of an aconitase-isocitrate complex, we successfully predicted the binding configuration of isocitrate. Four configurations were found, the energetically most favorable of which fit the observed electron density well and was used as a starting model for further refinement. Two configurations were found in citrate docking experiments, the second of which approximates the mode of substrate binding in an aconitase–nitrocitrate complex. We were also able to propose two binding modes of the catalytic intermediate *cis*-aconitate. These correspond closely to the isocitrate and the citrate binding modes. The relation of these new results to the proposed reaction mechanism is discussed.**

Key words: docking, active site, aconitase, structure prediction

INTRODUCTION

Mitochondrial aconitase [citrate (isocitrate) hydrolyase, EC4.2.1.3] is a textbook case for stereoselective reaction. In the second and third step of the Krebs cycle, aconitase catalyzes the stereospecific, reversible isomerization of citrate to isocitrate via the dehydrated intermediate *cis*-aconitate. Aconitase has been a popular target for biophysical and biochemical studies, in part because of the unusual observation that the [4Fe-4S] cluster of aconitase is not involved in a redox process, but instead in substrate selectivity and catalysis. In addition, the high identity of the amino acid sequence of aconitase and iron-responsive element binding protein (IRE-BP)—30% identity, 53% identity with conservative amino acid categories.[1]—has further focussed attention on aconitase. The highly conserved active site residues suggest that substrate binding and catalysis by IRE-BP is a part of its function as a translational regulatory molecule.

Spectroscopic studies on mitochondrial aconitase have focused on the structural and functional properties of the Fe-S cluster in different activation states.[2,3] Observable properties include: the reversible interconversion of a [3Fe-4S] cluster to a [4Fe-4S] cluster; cluster-ligation of carboxyl groups in the substrates citrate, *cis*-aconitate and isocitrate; and the coordination of water and hydroxyl molecules to the catalytically active [4Fe-4S] cluster.

Crystallographic studies of the inactive [3Fe-4S] form[4] and the active [4Fe-4S] form[5] of aconitase show four domains: the three amino terminal domains form a large subunit, connected to the fourth carboxy-terminal domain by a segment of random coil. The active site is trapped between the two halves. The Fe-S cluster is located at one end of the active site pocket, covalently linked to three cysteines in the amino terminal half. In the crystal of the active [4Fe-4S] enzyme, the fourth inequivalent iron site (Fe4) is exposed to solvent in the active site and coordinated by hydroxyl and the active site is occupied by sulfate. Crystallographic studies of aconitase complexed with the substrate isocitrate[6] and the inhibitor nitrocitrate[7] show the substrates coordinated to Fe4 via their hydroxyl oxygen and a

Received January 5, 1993; revision accepted April 15, 1993.
Address reprint requests to Dr. Arthur J. Olson, Department of Molecular Biology, The Scripps Research Institute, 10666 North Torrey Pines Road, La Jolla, CA 92037.

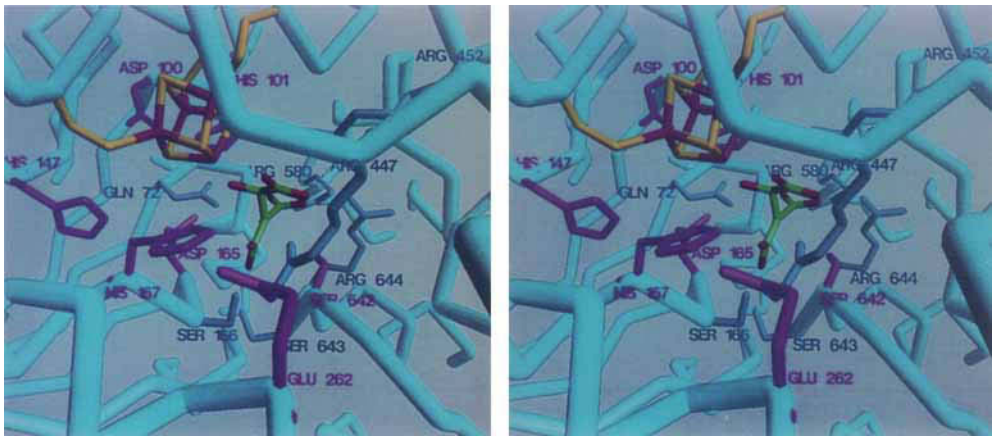

Fig. 1. Stereo view of the active site of aconitase. The bound isocitrate is shown in green and red at the center below the 4Fe-4S cluster. Side chains of the catalytic residues are shown in magenta, those side chains involved in recognition are shown in blue.

carboxyl oxygen. In each, a water molecule is also coordinated to the cluster. Residues from all four domains participate in aspects of the reaction: Gln-72, Ser-166, Arg-477, Arg-452, Arg-580, Ser-643, and Arg-644 in substrate recognition; Asp-100, His-101, His-147, Asp-165, His-167, Glu-262, and Ser-642 in catalysis; Ala-74, Asp-568, Ser-571, and Thr-567 in hydrogen bonding networks; and Asn-258, Cys-358, Cys-421, Cys-424, and Asn-446 in cluster ligation and interaction (Fig. 1).

Based on these structural data, a mechanism of aconitase catalysis has been proposed[6] and tested by site-directed mutagenesis.[8] Spectroscopic and kinetic characterization of mutants have provided evidence for four functional groups in the active site: Arg-580 appears to be a key residue in substrate binding, Asp-100 and His-101 appear to be involved in elimination of substrate hydroxyl, and Ser-642 appears to be the general base for proton abstraction/donation in the catalytic step.

To further probe the configurational preferences of the three substrates of aconitase—citrate, *cis*-aconitate, and isocitrate (Fig. 2)—we have employed an automated docking procedure. Our automated docking experiments have augmented the crystallographic work in two ways. In the early stages of crystallographic refinement, we were able to (successfully) predict the binding configuration of substrate in an aconitase-isocitrate complex, aiding in the interpretation of experimental substrate electron density. Second, we were able to explore the binding of a substrate which is difficult by crystallographic techniques: the transiently formed *cis*-aconitate intermediate.

METHODS

Automated Docking

The automated docking technique, described in full elsewhere,[9] starts with a substrate molecule in an arbitrary conformation and position, and finds favorable docked configurations in a protein active

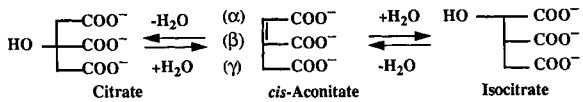

Fig. 2. Substrates of aconitase.

site. Simulated annealing is used for the configurational search. The substrate performs a random walk around the (static) protein. At each time step, the substrate is moved by a small increment in global translation and rotation and in each torsion angle. The new configuration is accepted or rejected probabilistically based on a temperature. The simulation is started at high temperature, allowing the substrate to move throughout the simulation space with little regard to unfavorable contacts. As the simulation proceeds, the temperature is reduced, slowly constraining the substrate to occupy only favorable regions. The initial high temperature phase allows the molecule to explore much of the simulation space and the final stages refine the best solutions. Energies are evaluated at each time step using a precalculated 3-D grid of interaction energies, similar to those of Goodford.[10]

Simulation Parameters

Interaction pseudoenergies are calculated with a molecular mechanics type of force field, including electrostatic, hydrogen bonding, and dispersion/repulsion terms. Substrates are restrained to ideal geometry, changing only in dihedral angles. The weights applied to electrostatic, hydrogen bonding and dispersion/repulsion terms are identical with those of the previous work.[9] Values were taken from AMBER,[11] and the 10–12 hydrogen bond coefficients scaled up by a factor of 10. The iron was also modeled by a 10–12 potential, with an energy minimum of −15 kcal/mol at a distance of 2.0 Å. Charges for the [4Fe-4S] cluster were taken from Noodleman et al.[12] Previously, docking simulations with these parameters successfully found the crys-

tallographic binding modes of several polar substrates. Coordinates for aconitase were taken from the refinement of the aconitase–isocitrate complex structure,[6] at the stage just before substrate was fit into the active site density.

Starting substrate coordinates were obtained from the Cambridge Crystallographic Data Bank and moved roughly into the protein active site. No attempt was made to align the substrates with protein atoms or experimental electron density; they were merely translated to place them in the empty space of the active site.

Two different docking schedules were tested. Most docking experiments were performed with a short docking schedule different than that used previously: 50 cycles each composed of 3,000 steps accepted or rejected, starting at a very high temperature (k_BT = 100 kcal/mol) and decreasing by a factor of 0.9 each cycle. For each substrate, two experiments, each with 100 individual docking simulations, were performed, each using a different seed value for random number generation. One started with the substrate orientation as roughly placed above, the second started with an orientation 180 degrees rotated about the x-axis. To check the efficacy of this docking schedule, isocitrate was also docked using the previously reported schedule: 10 docking simulations, each with 50 cycles of 30,000 steps accepted or rejected, with the same temperature parameters. A single experiment, including 10 simulations with the long schedule or 100 simulations with the short, required 5 to 10 hr to compute on a Convex C240, so our turnaround time was one experiment every day or two. The advantage of the shorter docking schedule is the increase in the number of simulations that can be performed in a reasonable amount of time, yielding a larger statistical base on which to validate the results.

RESULTS

Docking simulations were performed for the three substrates: isocitrate, *cis*-aconitate, and citrate. The two different simulated annealing schedules were tested with isocitrate; comparing the short schedule with the long schedule, we see little difference. Both schedules returned the same four configurations, and both the best of the two short simulations and the best of the two long simulations yielded configuration A as the preferred conformation, location and orientation of the ligand. Results are tabulated in Table I.

Each substrate yielded a consistent set of two to four configurations. Each configuration was found in multiple docking simulations. The predominant force in determining the optimal configurations was hydrogen bonding interaction between substrate carboxyl oxygens and surrounding amino acids. With the force field described above, the hydrogen bonding interactions generally totalled two to three times the total interaction pseudoenergy of coordination with Fe4. The simulated orientations differ in which of the three carboxyls is coordinated to the [4Fe-4S] cluster and where the remaining two carboxyls find optimal hydrogen binding sites with surrounding amino acids. Crystallographic studies show that isocitrate coordinates via its hydroxyl oxygen and its α-carboxyl. Spectroscopy reveals that citrate coordinates via its hydroxyl oxygen and β-carboxyl and that *cis*-aconitate coordinates via its α-carboxyl or β-carboxyl, depending on its binding mode. The simulated binding orientations that are consistent with these results are given special attention in the following discussions.

Isocitrate

Four isocitrate configurations were found, shown in Figure 3 relative to the active site [4Fe-4S] cluster. Each is coordinated to Fe4 by one carboxyl oxygen—the α-carboxyl in A, the β-carboxyl in C, and the γ-carboxyl in B and D—and the energetically most favorable configuration (A) is also coordinated at the hydroxyl oxygen. The remaining carboxyl and hydroxyl oxygens in each case are extensively hydrogen bonded to protein atoms. Configurations A, B, and C are related to each other by an approximate 120 degree rotation about the horizontal axis of the figure, successively bringing different carboxyls into contact with the FeS cluster. Configuration D is approximately related to configuration C by a rotation of 180 degrees in the vertical axis of the figure, with major changes of dihedral angles (notice the different orientation of the central chiral carbon atom in D versus A, B, and C).

All four configurations were compared to the experimental electron density of the aconitase–isocitrate complex. Configuration A unabiguously fit the observed density, the other configurations did not; configuration A was then used as the starting point for further crystallographic refinement.[6] For reference, the crystallographic orientations of isocitrate and nitrocitrate are shown in Figure 6.

Isocitrate configuration A is functionally identical with the crystallographic isocitrate configuration. It binds in the active site via ligation of hydroxyl and one α-carboxyl oxygen to Fe4. The α-carboxyl is also within hydrogen bonding distance to the sidechain of Arg-447 and Arg-452. The hydroxyl is also within hydrogen bonding distance to the ε-nitrogen of His-101 and the carboxyl of Asp-165. The β-carboxyl forms hydrogen bonds with the mainchain amide nitrogen of Ser-166, the hydroxyls of Ser-166, Ser-642, and Ser-643, and side chain of Arg-447. The γ-carboxyl interacts with sidechain of Arg-580 and Arg-644 and the hydroxyl of Ser-642.

Citrate

Two configurations of nearly identical pseudoenergy were found for citrate, shown in Figure 4. Configuration A is coordinated to iron through the hydroxyl and the γ-carboxyl, and configuration B is

TABLE I. Results of Docking

System*	Rank†	Pseudoenergy range	No. of solutions‡	Configuration
Isocitrate				
Short schedule 1	1	−83.62 to −76.31	36	A
	3	−82.37 to −77.11	18	D
	10	−81.47 to −77.00	7	B
	13	−80.98 to −72.55	8	C
	54	−78.05 to −69.30	31/10	Other
Short schedule 2	1	−84.05 to −77.44	24	A
	3	−82.44 to −71.06	16	B
	8	−81.63 to −74.79	20	C
	21	−80.30 to −78.35	3	D
	32	−79.42 to −69.71	37/9	Other
Long schedule 1	1	−82.70 to −80.62	3	B
	3	−81.60 to −78.81	4	A
	4	−81.35	1	C
	5	−81.34 to −80.47	2	D
Long schedule 2	1	−84.00 to −79.04	6	A
	5	−81.47 to −80.53	3	B
	7	−81.10	1	C
Citrate				
Short schedule 1	1	−87.86 to −79.18	26	A
	3	−87.28 to −81.47	25	B
	46	−83.29 to −67.65	49/5	Other
Short schedule 2	1	−89.06 to −82.12	29	A
	2	−88.09 to −82.64	29	B
	59	−81.57 to −69.22	42/6	Other
cis-aconitate				
Short schedule 1	1	−78.70 to −75.58	20	A
	17	−75.81 to −71.36	9	C
	21	−75.43 to −72.32	44	D
	22	−75.24 to −68.99	22	B
	65	−72.87 to −70.99	5/2	Other
Short schedule 2	1	−78.83 to −76.04	18	A
	18	−76.38 to −67.92	17	B
	20	−75.66 to −69.93	8	C
	22	−74.92 to −72.44	33	D
	52	−72.93 to −65.94	24/4	Other

*Short docking schedules are composed of 100 simulations, each with 50 constant temperature cycles, each with a maximum of 3,000 time steps accepted or rejected. The temperature started at a high value ($k_BT = 100$ kcal/mol) and reduced by a factor of 0.9 each cycle. Long docking schedules are composed of 10 simulations, each with 50 cycles of 30,000 steps. Schedules 1 and 2 in each experiment are identical, except that the starting orientation of the substrate was changed by 180 degrees around the x-axis.
†Rank of top solution, out of 100 for short schedules, out of 10 for long schedules.
‡Configurations were scored as identical if the carbon atoms differed by no more than 1 Å from the top solution. The high energy configurations in each simulation are not tabulated separately—all are grouped as a low ranked set. The entry 31/10 refers to 31 simulations in 10 different configurations.

coordinated through the hydroxyl oxygen, with a long interaction between Fe4 and the β-carboxyl. Configuration A is approximately related to configuration B by a 120 degree rotation about the hydroxyl bond. Citrate configuration A is most similar to isocitrate configuration D; citrate configuration B has no counterpart in the isocitrate results.

Citrate configuration B is similar to the crystallographic configuration of nitrocitrate,[13] a citrate isostere. In our model, it binds in the active site via ligation of hydroxyl. The β-carboxyl is rotated away from the cluster, with closest contact of 3.5 Å between carboxyl oxygen and Fe4, forming hydrogen bond interactions with side chains of Arg-447, Arg-452, and Arg-644.

The configuration of citrate found in our previous study,[9] using protein coordinates from the crystallographic determination of aconitase alone, does not correspond to either of these citrate binding modes.

cis-Aconitate

cis-Aconitate is perhaps the most interesting substrate for docking experiments; it has not been possible to cocrystallize the enzyme with this sub-

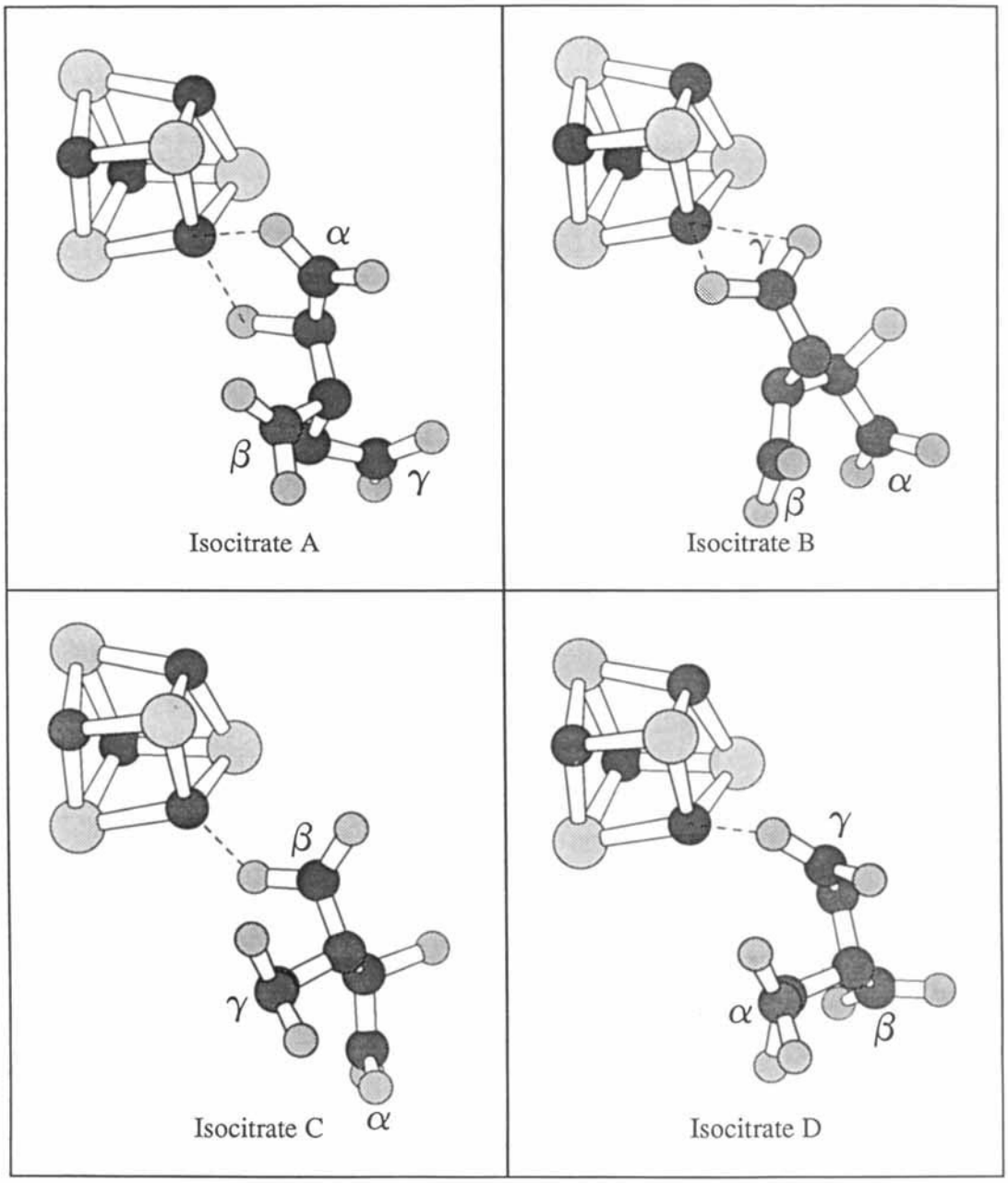

Fig. 3. Isocitrate docking results. Four configurations of isocitrate were found, shown here in the same orientation as Figure 1, relative to the protein [4Fe-4S] cluster. In the substrate, carbon is dark and oxygen light; in the cluster, iron is dark and sulfur light. Coordination from substrate oxygen to Fe4 is shown as a dotted line. This and the following three figures were calculated with Molscript.[15]

strate.[6] The docking results are provocative: four orientations were obtained, shown in Figure 5, two of which strongly resemble the crystallographically observed modes of binding of isocitrate and nitrocitrate. Configuration A is the configuration of most favorable energy. It is similar in character to citrate configuration B and the observed mode of binding of nitrocitrate, with the β-carboxyl coordinated to iron. Configurations B, C, and D all have comparable pseudoenergies, several kcal/mol less favorable than that of configuration A. Configuration C of *cis*-aconitate is similar to the A configuration of isocitrate, with α-carboxyl coordination. Coordinates of configurations A and C—the putative reactive binding modes—are included in Table II, in the coordinate frame of the isocitrate–aconitase complex.

cis-Aconitate configuration A is a model for the citrate binding mode of *cis*-aconitate. It is coordi-

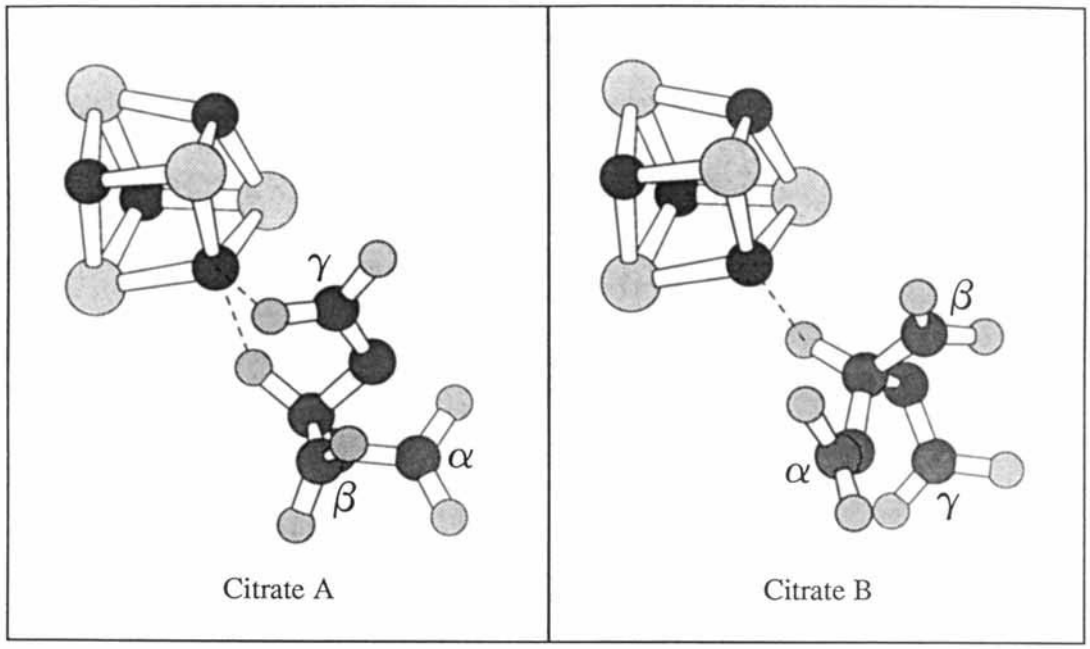

Fig. 4. Citrate docking results. The two configurations of citrate are shown, in the same orientation as Figure 3. Note that citrate is not a chiral molecule—the α and γ carboxyls, labeled here to be consistent with the isocitrate binding mode, are equivalent until the enzyme discriminates one particular binding mode.

nated to Fe4 by one β-carboxyl; the second β-oxygen orients toward the side chain amines of Arg-452 and Arg-644. The α-carboxyl interacts with side chain hydroxyl and main chain amide nitrogen of Ser-166 and Ser-643. The α-carboxyl also interacts with the hydroxyl of Ser-642, the δ-nitrogen of His-167, and carboxyl oxygen of Asp-165. Strong hydrogen bonding interactions occur between the β-carboxyl and an amine of Arg-447. The γ-carboxyl forms hydrogen bonds with the amines of Arg-580 and the amide nitrogens of Arg-644 and Gln-72. The α-carbon of *cis*-aconitate (the site of proton addition in the isocitrate to citrate reaction) is in close proximity to the hydroxyl of Ser-642 and carboxyl oxygen of Asp-165.

cis-Aconitate configuration C is a model for binding in the isocitrate binding mode. One oxygen of the α-carboxyl is coordinated to Fe4 and the other is hydrogen bonded to the guanidinum nitrogens of Arg-452 and Arg-447. The β-carboxyl group is hydrogen bonded with the backbone amide nitrogen of Ser-166 and the hydroxyls of Ser-642 and Ser-643, and is in close contact with the carboxyl of Asp-165. The γ-carboxyl points to the other end of the active site, interacting with the amino nitrogens of Arg-580, Gln-72, and Arg-644 and the hydroxyl of Ser-642.

Water

Fe4 is octahedrally coordinated in the crystallographic structure of both the isocitrate complex and the nitrocitrate complex. In both cases, three positions are filled by sulfur in the cluster, two positions are occupied by substrate carboxyl and hydroxyl oxygens, and the sixth is occupied by a water molecule. To test the consistency of the predicted *cis*-aconitate complex with these experimentally observed results, we calculated a grid of interaction pseudoenergies using the model *cis*-aconitate:aconitase complexes, with water as a probe. The results are shown in Figure 7.

Both of the predicted configurations of *cis*-aconitate are coordinated to Fe4 at a single carboxyl oxygen, leaving two free coordination sites. The grid of interaction energies clearly shows regions of favorable potential at both of these free sites. The front peak in the figures corresponds closely to the observed water coordination site in the crystallographic structures. The hind peak is postulated to be the water abstracted during catalysis. Its position corresponds closely to the position of the hydroxyl in both the isocitrate complex and the nitrocitrate complex.

It is somewhat surprising that these two peaks were resolved so cleanly, since our grid calculation uses a spherical potential around each atom. The sharp localization of the two peaks is due to the combination of the favorable interaction with Fe4 and several favorable interactions with neighboring protein side chains. The front position forms hydrogen bonds with His-167 and Asp-165, the hind position forms hydrogen bonds with His-101 and Asp-165.

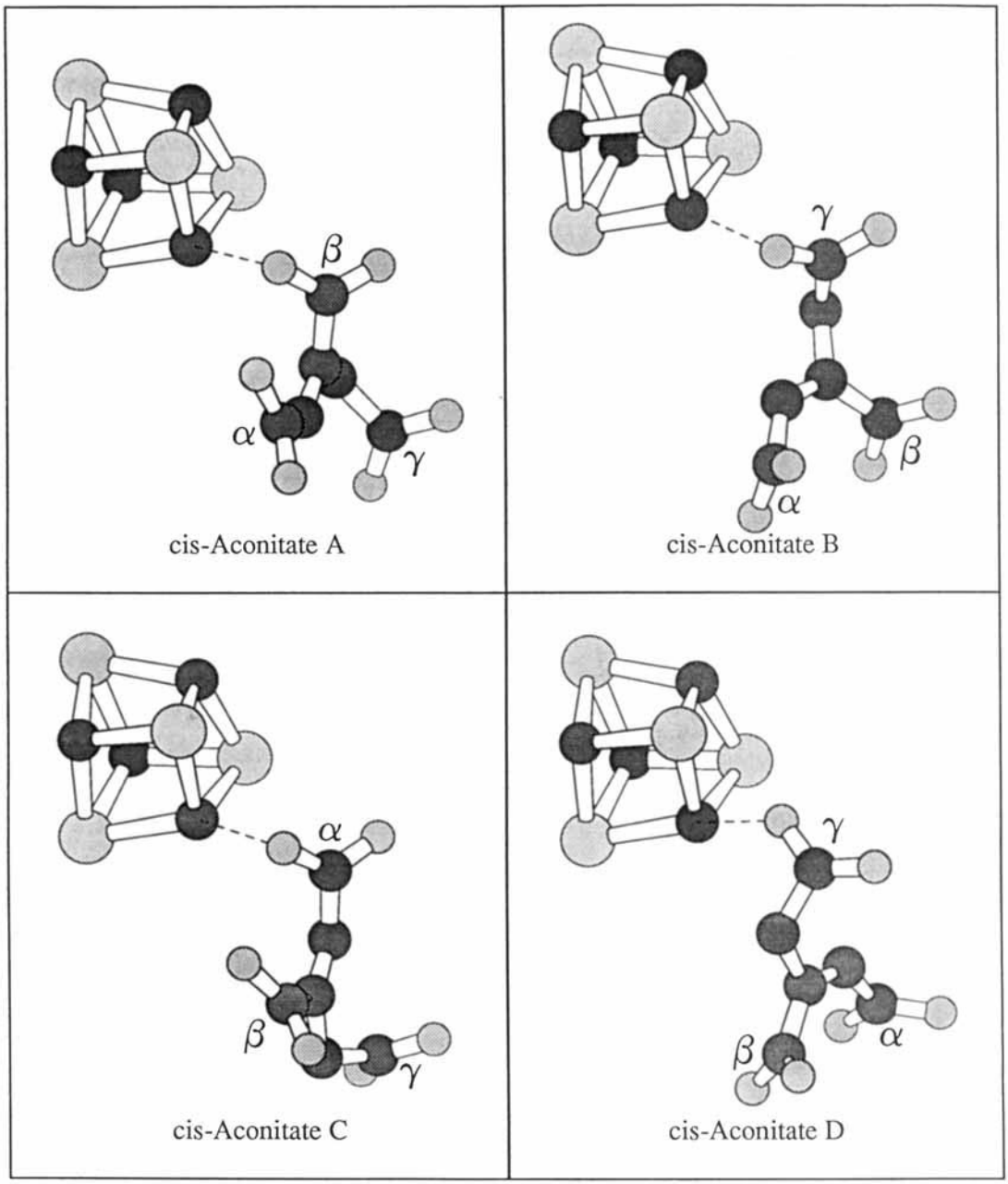

Fig. 5. *cis*-Aconitate docking results. The four configurations of *cis*-aconitate are shown, in the same orientation as Figure 3.

DISCUSSION

Aconitase is an ideal system for application of the automated docking protocol. All 22 active site residues are closely packed at the interface of the two aconitase subunits, forming an active site of limited extent—in fact, a totally enclosed active site. This substantially reduces the configurational space to be searched. The crystallographic coordinates of aconitase with two different substrates show excellent superposition, with root mean square deviation of protein atoms of 0.185 Å.[6] The minimal conformational change of active site residues upon ligand binding in these two structures suggests that our calculations, with different substrates in the same active site model, are appropriate.

The simulated isocitrate orientation mirrors the crystallographic structure determination, reproducing the main features of hydrogen bonding and coordination. The simulated citrate configuration is consistent with the crystallographically determined position of the analogue nitrocitrate, preserving the

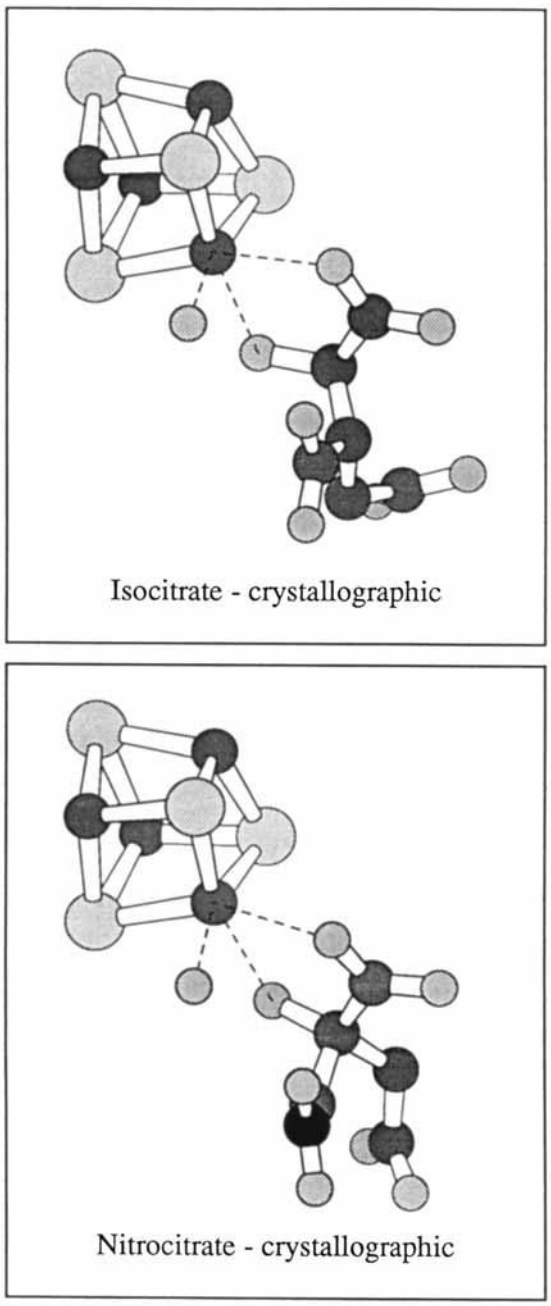

Fig. 6. Crystallographic configurations of isocitrate and nitrocitrate. Shown in the same orientation as Figure 3.

orientation and coordination, but differing slightly in details of placement in the α- and γ-carboxyls. The two *cis*-aconitate binding orientations are virtually identical to the crystallographic binding modes of isocitrate and nitrocitrate, with slight rearrangements necessitated by the rigid *cis* bond, giving us confidence that these two orientations are reasonable models for the catalytic states.

The two modeled binding modes of *cis*-aconitate fit nicely into the accepted scheme of the aconitase reaction. Elimination of the α-hydroxyl and abstraction of the β-proton from isocitrate forms *cis*-aconitate in the isocitrate binding mode. In our model, this dehydration merely shifts the α-carboxyl and the β-carboxyl relative to the isocitrate position. Coordination of the α-carboxyl and hydrogen bonding interactions with the surrounding active site amino acids are structurally conserved.

The simulated orientations of citrate and *cis*-aconitate in the citrate binding mode reveal slightly larger rearrangements upon reaction. Hydration of *cis*-aconitate to citrate causes an approximate 20 degree rotation of the molecule, allowing the citrate hydroxyl to coordinate with Fe4, but increasing the distance between the β-carboxyl and Fe4 to 3.5 Å. This distance is consistent with the nitrocitrate crystal results, where the distance is 3.3 Å.[13] The β-carboxyl in citrate is stabilized in this new conformation by increased hydrogen bonding with surrounding arginine residues.

The orientation of the α- and β-carboxyls of the two simulated binding modes of *cis*-aconitate provide an explanation for the observed stereospecific conversion of α-methyl-*cis*-aconitate into α-methyl-isocitrate, and not to α-methyl-citrate.[14] In the citrate binding mode, the methyl group would make unacceptable contact with Asp-165. In the isocitrate binding mode, however, no unacceptable contacts with protein atoms are formed (data not shown).

The interconversion of citrate and isocitrate by aconitase requires *cis*-aconitate to dissociate and reassociate in a different configuration, changing from the isocitrate mode to the citrate mode, or vice versa. In our model, the two modes have striking structural similarities. The β-carboxyl oxygens in the citrate-binding mode superimpose with the α-carboxyl oxygens of the isocitrate mode, in identical coordination with Fe4 and hydrogen bonding with adjacent residues. The α-carbon and β-carbon in the citrate binding mode virtually superimpose with the β-carbon and α-carbon of the isocitrate binding mode, respectively (rmsd = 0.15 Å). This configuration conserves the functional proton abstraction/donation interaction with the hydroxyl of ser-642. This configuration is also compatible with the abstraction and donation of water coordinated to Fe4, as modeled by the water affinity maps shown in Figure 7.

CONCLUSIONS

Automated docking has aided in the structural analysis of aconitase on two grounds. First, the procedure generated a small number of starting models for substrates, using only protein coordinates from an early stage of refinement (these predicted substrate configurations were, as is true with most theoretical work, completely unbiased by data). For isocitrate, a starting model was chosen from the several possibilities by simple visual inspection on an

TABLE II. *cis*-Aconitate Docked Coordinates

REMARK *cis*-aconitate configuration A								
ATOM	1	CCG	CAC	A	1	38.246	35.312	72.076
ATOM	2	CG	CAC	A	1	37.779	34.317	71.004
ATOM	3	CB	CAC	A	1	36.291	34.274	70.844
ATOM	4	CA	CAC	A	1	35.538	34.040	71.934
ATOM	5	CCA	CAC	A	1	34.075	33.892	72.139
ATOM	6	CCB	CAC	A	1	35.796	34.492	69.424
ATOM	7	OG1	CAC	A	1	38.148	36.529	71.765
ATOM	8	OG2	CAC	A	1	38.678	34.881	73.156
ATOM	9	OA1	CAC	A	1	33.640	34.124	73.270
ATOM	10	OA2	CAC	A	1	33.307	33.506	71.176
ATOM	11	OB1	CAC	A	1	36.205	35.471	68.799
ATOM	12	OB2	CAC	A	1	34.959	33.662	68.90
TER								
REMARK *cis*-aconitate configuration C								
ATOM	1	CCG	CAC	C	1	37.824	35.048	73.152
ATOM	2	CG	CAC	C	1	36.608	34.117	73.267
ATOM	3	CB	CAC	C	1	35.756	34.105	72.037
ATOM	4	CA	CAC	C	1	36.344	34.333	70.849
ATOM	5	CCA	CAC	C	1	35.820	34.434	69.463
ATOM	6	CCB	CAC	C	1	34.279	33.842	72.287
ATOM	7	OG1	CAC	C	1	38.939	34.515	73.396
ATOM	8	OG2	CAC	C	1	37.650	36.236	72.834
ATOM	9	OA1	CAC	C	1	36.300	35.314	68.744
ATOM	10	OA2	CAC	C	1	34.882	33.649	69.052
ATOM	11	OB1	CAC	C	1	33.742	34.374	73.258
ATOM	12	OB2	CAC	C	1	33.625	33.071	71.491
TER								

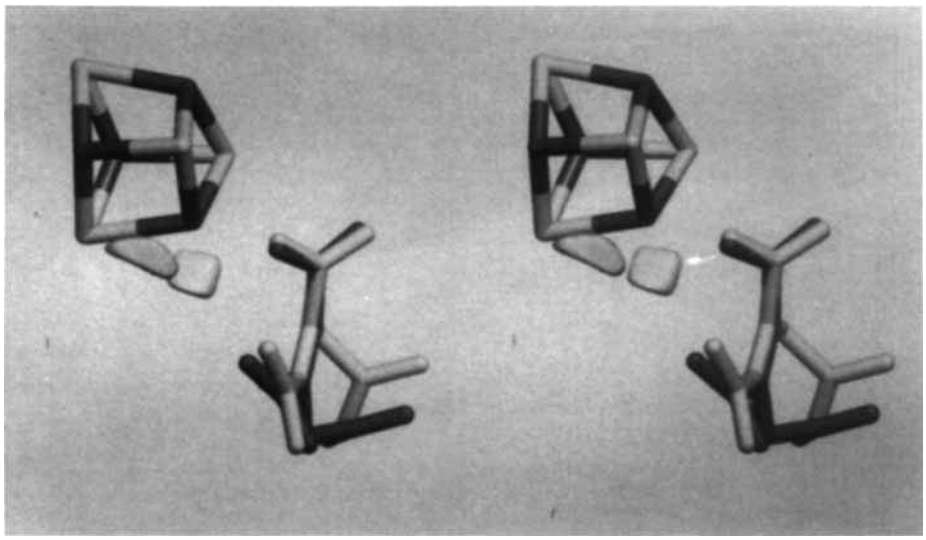

Fig. 7. Stereo figure of water interaction pseudoenergy in the model *cis*-aconitate:aconitase complexes, using *cis*-aconitate configuration A. Interaction pseudoenergies for a water probe are volume rendered[16] in the same orientation as the preceding figures, with a contour at −2.5 kcal/mol. Contours calculated using *cis*-Aconitate configuration C are virtually identical. *cis*-Aconitate is shown in both the citrate binding mode (light bonds) and the isocitrate binding mode (dark bonds). The front peak corresponds to the observed crystallographic water in the isocitrate complex, the rear peak occupies the position of the hydroxyl in the isocitrate and nitrocitrate structure determinations.

interactive graphics screen: one configuration fit very well, the others were obviously misplaced. Second, automated docking provided a method for exploring aspects of catalysis inaccessible to crystallography: in this case, the unobserved *cis*-aconitate complex.

The utility of this technique is not limited to the aconitase system. Automated docking may be used for the prediction of intermediate substrate-binding modes in any enzyme of known structure. The major limitation to the current technique is the use of a static protein structure: one must assume that the active site of the enzyme during catalysis may be modeled by the active site of the enzyme in crystallographically observed states.

ACKNOWLEDGMENTS

The authors thank H. Beinert and M. C. Kennedy for helpful comments on the manuscript. This work is funded in part by Grant PO1GM38794 from the National Institute of Health and a grant from Johnson and Johnson.

REFERENCES

1. Roualt, T.A., Stout, C.D., Kaptain, S., Harford, J.B., Klausner, R.D. Structural relationship between an iron-regulated RNA-binding protein (IRE-BP) and aconitase: Functional implications. Cell 64:818–883, 1991.
2. Emptage, L. Q., ed. "Metals Cluster in Proteins." Washington, DC: American Chemical Society, 1988: 343–371.
3. Cammack, R., ed. Aconitase: An iron-sulfur enzyme. In: "Advances in Inorganic Chemistry, Iron Sulfur Proteins," Vol. 38. San Diego: Academic Press, 1992: 323–338.
4. Robbins, A.H., Stout, C.D. The structure of aconitase. Proteins 5:289–312, 1989.
5. Robbins, A.H., Stout, C.D. Structure of activated aconitase: Formation of the [4Fe-4S] cluster in the crystal. Proc. Natl. Acad. Sci. USA 86:3639–3643, 1989.
6. Lauble, H., Kennedy, M.C., Beinert, H., Stout, C.D. Crystal structure of aconitase with isocitrate and nitrocitrate bound. Biochemistry 31:2735–2743, 1992.
7. Lauble, H., Kennedy, M.C., Beinert, H., Stout, C.D. Crystal structures of aconitase with trans-aconitate and nitrocitrate bound. J. Mol. Biol., Submitted.
8. Zheng, L., Kennedy, M.C., Beinert, H., Zalkin, H. Mutational analysis of active site residues in pig heart aconitase. J. Biol. Chem. 267, 7895–7903, 1992.
9. Goodsell, D.S., Olson, A.J. Automated docking of substrates to proteins by simulated annealing. Proteins 8:95–202, 1990.
10. Goodford, P.J. A computational procedure for determined energetically favorable binding sites on biologically important molecules. J. Med. Chem. 28:849–857, 1985.
11. Weiner, S.J., Kollman, P.A., Case, D.A., Singh, U.C., Ghio, C., Alagona, G., Profeta, S., Weiner, P. A new force field for molecular mechanical simulation of nucleic acid and protein. J. Am. Chem. Soc. 106:765–784, 1984.
12. Noodleman, L., Norman, J.G. Jr., Osborne, J.H., Aizman, A., Case, D.A. Models for ferredoxins: Electronic structures of iron-sulfur clusters with one, two, and four iron atoms. J. Am. Chem. Soc. 107:3418–3426, 1985.
13. Lauble, H., Kennedy, M.C., Beinert, H., Stout, C.D., unpublished data.
14. Schloss, J.V., Emptage, M.H., Cleland, W.W. pH Profiles and isotope effects for aconitases from *Saccharomycopsis lipolytica*, beef heart, and beef liver. α-Methyl-*cis*-aconitate and *threo*-D_s-α-Methylisocitrate as substrates. Biochemistry 23:4572–4580, 1984.
15. Kraulis, P.J. MOLSCRIPT: A program to produce both detailed and schematic plots of protein structures. J. Appl. Crystallogr. 24:946–950, 1991.
16. Goodsell, D.S., Mian, I.S., Olson, A.J. Rendering volumetric data in molecular systems. J. Mol. Graphics 7:41–47, 1989.